



RESEARCH ARTICLE

Contribution to A Study of Some Seismic Observations Through the $(\text{Fe}_x\text{Ca}_{(1-x)})\text{O}$ Compounds up to the Limits of the Earth's Outer Core by Calculation

Noura Mebrouki¹, Salah Tlili^{2*}, Mohammed Said Nedjimi³, Azeddine Mazouz⁴, Mohamedhafed Berrebeuh⁵

¹ LRPPS Laboratory, Faculty of Mathematics and Material Sciences, KasdiMerbah Ouargla University, Ouargla, Algeria

^{2,5} LARENZA Laboratory, Faculty of Mathematics and Material Sciences, KasdiMerbah Ouargla University, Ouargla, Algeria

³ Institution: VPRS Laboratory, Faculty of Mathematics and Material Sciences, KasdiMerbah Ouargla University, Ouargla, Algeria

⁴ Faculty of Material Sciences, Batna University, Batna, Algeria

ARTICLE INFO**ABSTRACT**

Received: Jul 19, 2024

Accepted: Sep 21, 2024

Keywords

Seismic Observations

Prem Model

Hashin & Shtrikman Relationships

Compounds $(\text{Fe}_x\text{Ca}_{(1-x)})\text{O}$

Iron Oxide

Calcium Oxide

Based on our previous computational studies, we were determined a change in the initial cell volume, shear and bulk modulus at the pressures of the PREM model for both iron and calcium oxides and using the relationship between seismology and metallurgy and Hashin & Shtrikman relationships. This work enabled us to study the most important seismic observations, namely the compounds density, the values of shear and bulk modulus, longitudinal, transversal and bulk sound waves velocities, which are specific to minerals of the form $(\text{Fe}_x\text{Ca}_{(1-x)})\text{O}$ at the pressures of this model representative of the Earth's material, moreover, the ratio x was changed from a percentage to a hundred thousand. We were got the values of those studied parameters, especially at the most important limits between the Earth's internal layers until to the limits of the Earth's outer core. The unclear compounds that exist indeed in the Earth's layers, but with no coordination in those values between all parameters, with confirmation of the presence of iron oxide from 1571 km to the last depth. We were also found that the increase in the accuracy of the iron ratio in the studied compounds from percentage to more accurate, confirms that it is mostly effective. And this is not the case except in some very few domains, with the exception of the density, in which this accuracy is effective on all domains.

***Corresponding Authors:**

tlililah2007@gmail.com

1. INTRODUCTION

Density, longitudinal and transversal waves velocity is considered important seismic observations (Kennett, B. L. N. 2006), that is because of the possibility of comparing it with its counterpart known about the Earth's material through its available value in the PREM model (Dziewonski, A. M., & Anderson, D. L. 1981). Therefore, density is the only one of the structural properties, which is included in these observations (Bolt, B., B K. 1985). While can't consider those two waves velocities

alone among the elastic properties, which is included in those observations (Bullen, K. E., & Bolt, B. A. 1985). Only through their values can the bulk sound wave velocity be calculated, and on the other hand, depending on the knowledge of the density value, both the bulk and the shear modulus can be calculated (Poirier, J. P. 2000). Or vice versa, depending on the two values of these two parameters and the density value, the value of the two velocities of the first two waves can be calculated, and therefore the velocity of the third wave can be deduced (Baddari, K. 1994).

Table 1: Values of the depth number, its value, the corresponding pressure, the density of the Earth's material, and the velocities of the longitudinal and transversal waves at each depth extracted by the PREM model in the most important Earth intervals up to the boundaries of the outer core of the earth.

	Pressure value	Depth (Km)	Pressure (GPa)	Densityn (g/cm^3)	Longitudinal wave velocity (Km/s)	Transversal wave
Earth's crust	1	0	0	1,02	1,44996	0
	2	3	0,0299	1,02	1,44996	0
	3	3	0,0303	2,6	5,79328	3,19101
	4	15	0,3364	2,6	5,79328	3,19101
	5	15	0,337	2,9	6,79151	3,88904
	6	24,4	0,604	2,9	6,79151	3,88904
	7	24,4	0,6043	3,30076	8,10074	4,47863
	8	40	1,1239	3,37906	8,09135	4,47253
	9	60	1,7891	3,37688	8,07928	4,4648
	10	80	2,4539	3,37471	8,06715	4,45717
Upper mantle	11	80	2,4546	3,37471	8,00468	4,37682
	12	115	3,6183	3,37091	7,98383	4,36344
	13	150	4,7824	3,3671	7,96278	4,35034
	14	185	5,9466	3,3633	7,94153	4,33752
	15	220	7,1108	3,3595	7,92008	4,32499
	16	220	7,1115	3,43578	8,5192	4,58914
	17	265	8,5497	3,46264	8,60561	4,62027
	18	310	10,2027	3,48951	8,69204	4,65139
	19	355	11,7702	3,51639	8,77848	4,68252
	20	400	13,352	3,54325	8,86489	4,71364

	21	400	13,3527	3,72378	9,09193	4,87442
	22	450	15,2251	3,78678	9,34655	5,01854
	23	500	17,1311	3,8498	9,60122	5,16268
	24	550	19,0703	3,91282	9,85588	5,30682
	25	600	21,0425	3,97584	10,11055	5,45095
	26	600	21,0426	3,97584	10,11055	5,45097
	27	635	22,4364	3,98399	10,16454	5,47775
	28	670	23,8334	3,99214	10,21852	5,50452
Lowermantle	29	670	23,8342	4,38071	10,72743	5,91294
	30	721	26,0783	4,41241	10,88533	6,06124
	31	771	28,2927	4,44316	11,04001	6,20672
	32	771	28,2928	4,44317	11,04002	6,20673
	33	871	32,7623	4,50372	11,21918	6,2768
	34	971	37,2852	4,56304	11,38972	6,34365
	35	1071	41,8606	4,62129	11,55225	6,40749
	36	1171	46,4882	4,67844	11,70739	6,46855
	37	1271	51,1676	4,7346	11,85576	6,52702
	38	1371	55,8991	4,78983	11,99798	6,58313
	39	1471	60,683	4,84422	12,13466	6,6371
	40	1571	65,5202	4,89783	12,26642	6,68912
	/	1671	70,4119	4,95073	12,39389	6,73943
	/	1771	75,3598	5,00299	12,51767	6,78823
	41	1871	80,366	5,05469	12,63839	6,83574
	42	1971	85,4332	5,1059	12,75667	6,88216
	43	2071	90,5646	5,15669	12,87311	6,92772
	44	2171	95,7641	5,20713	12,98835	6,97264
	45	2271	101,036	5,25729	13,10299	7,01711
	46	2371	106,386	5,30724	13,21765	7,06136
	47	2471	111,820	5,35706	13,33296	7,10561
48	2571	117,346	5,40681	13,44953	7,15006	
49	2671	122,971	5,45657	13,56798	7,19492	

50	2741	126,974	5,49145	13,65234	7,2267
51	2741	126,974	5,49145	13,65234	7,2267
52	2771	128,706	5,50642	13,65949	7,22647
53	2871	134,561 9	5,55641	13,68369	7,22559
54	2891	135,750 9	5,56645	13,68862	7,22538

These observations are important in seismology the globe, which is a branch of seismology (Stein, C. A. 1991). This importance lies that it confirms the possibility of the presence of material elements in the depths of the Earth's interior or not, based on seismic models (Shearer, P. M. 2009). These models which the PREM model is considered one of the most important, due to its many uses. In addition, it provides a clear division of the Earth's internal layers in terms of their depth, corresponding pressure and the values of those observations previously mentioned, as they are recorded in Table (1) until to the limits of the Earth's outer core (Volgyesi, L., & Moser, M. 1982).

The Earth's internal layers consist mainly of many electrodes or oxides such as: MgO, BaO, CaO, FeO and others (Karki BB, Stixrude L, Wentzcovitch RM. 2001), And in turn, if they overlap with each other, they form many minerals, such as; Péridotites, Olivine, Pyroxène, spinelle, magnésiwüstite and others (Jackson, I. (Ed.). 2000). The thermodynamic conditions of these layers, such as pressure and temperature control the present phases, whether for oxides or minerals (Murakami M., et al. 2004). Many studies have been conducted in order to examine these materials in various ways, however experimental or computational. The latter are not mostly dependent on temperature change, most of it depends on a calculation in which the temperature is nonexistent (Louail, L. et al. 2006).

It is worth mentioning there are several studies that have addressed iron and calcium oxides, especially by changing the pressure up to 140 GPa, most of them have addressed the structural and elastic properties. One of the most important is the study of Tlili, S et al. 2017 for the first oxide, the study of Benatallah, N et al 2023 for the second oxide. Which confirmed phase stability B1 or type NaCl, before pressure 77 GPa and 59.2 GPa respectively. After that, the first oxide turns into the B8 phase of the NiAs type, while the second oxide turns into the B2 phase of the CsCl type. Moreover, although the second study (Benatallah, N et al 2023) was able to learn about the change of all the parameters studied within it, in particular those mentioned above on each pressure change domain, the first study (Tlili S, et al. 2017) did not recognize what was happening to the change of those parameters in the domain from 70 to 80 GPa.

However, It is noteworthy that no study has addressed the compounds resulting from the combination of these two oxides, where the dissolution of iron x in calcium oxide can be considered to produce minerals of the form $(\text{Fe}_x\text{Ca}_{(1-x)})\text{O}$. In this paper we will present a study of seismic observations up to the limits of the Earth's outer core special of these compounds, by changing x in percentages in the base and noting the exact change in its change in the ratio from a thousand to a hundred thousand. This is in a purely computational way and based on some of the results of the last two studies and special Hashin&Shtrikman relationships (Mattern, E. 2005), which are further explained in the next step. This is followed by an explanation of the results and finally a summary of the most important of these results presented.

2. METHOD OF STUDY

Regardless of the multiple computational methods, including so-called "ab-initio" methods based on partial dynamics (Marx, D., & Hutter, J. 2000), methods based on statistical physics (seismic methods)

(Poirier, J. P. 2000; Shearer, P. M. 2009) and methods based on thermodynamics (Kumar, M. 2002). The studies of Tlili, S et al. 2017 and Benatallah, N et al 2023 were based on the application of the density functional theory (DFT), which is one of the most important methods used in theoretical physics and chemistry, and is one of the most used in quantum calculations to solve Schrödinger's equation because of its applicability to diverse systems (multi-variable) (Segall, M. et al. 2002). CASTEP is based on this theory (Segall, M. et al. 2002), which in fact uses many approximations. Which became more accurate was the generalized gradient approximation (GGA) (Perdew, J. P., &Zunger, A. 1981; Perdew, J. P., Burke, K., &Ernzerhof, M. 1996), which developed and increased strength for its multiple uses possibilities, with the first study using the PW91 approximation (Perdew, J. P., &Zunger, A. 1981; Perdew, JP, et al. 1992) while the second study used PBEsol (Perdew, J. P., et al. 2008).

To determine the values of the studied parameters at the pressures of the PREM model, the second study (Benatallah, N et al 2023) adopted the mathematical approximation used for the polynomials expressing the change of any function within a particular interval, which is the pattern often known as generation or polarization (Werner, W 1984).). While we rely on determining the parameters values at the same pressures for iron oxide the same approximation, but it is based on linear polynomials between each two points addressed in the first study (Tlili, S et al. 2017).

Finally, to determine the parameters values required in the study for mineral compounds of the form (Fe_xCa_(1-x))O, based on mineralogy (Sobolev, SV., Babeyko, AY. 1994) the volume fraction of the mineral is calculated using the following relationship:

$$v_i = \frac{(x_{FeO}V_{FeO} + (1 - x_{FeO})V_{CaO})}{V} \quad (01)$$

where V is the size of the conventional cell volume which is deduced by conservation of mass as follows (Radovic, M., Lara-Curzio, E., Riester, L. 2004):

$$V = x_{FeO}V_{FeO} + (1 - x_{FeO})V_{CaO} \quad (02)$$

Thus, density values are determined by the relationship from mineralogy as follows (Sobolev, SV., Babeyko, AY. 1994):

$$\rho = \frac{1}{V}(x_{FeO}M_{FeO} + (1 - x_{FeO})M_{CaO}) \quad (03)$$

where V_i, x_i and v_i are respectively; molar volume, molar mass and molar fraction.

Hashin&Shtrikman's relationships enable (Mattern, E.2005) to calculate only both bulk and shear modulus, where:

For the shear modulus:

$$G_{HS} = \frac{G_{HS-} + G_{HS+}}{2} \quad (04)$$

where:

$$G_{HS-} = G_1 + \frac{B_1}{1 + \beta_1 B_1} \quad (05)$$

and

$$G_{HS+} = G_N + \frac{B_N}{1 + \beta_N B_N} \quad (06)$$

B₁ and B_N are calculated as follows:

$$B_1 = \frac{v_N}{[2(G_N - G_1)]^{-1} - \beta_1} \quad (07)$$

$$B_N = \frac{v_1}{[2(G_1 - G_N)]^{-1} - \beta_N} \quad (08)$$

$$\beta_1 = \frac{-3(K_1 + 2G_1)}{5G_1(3K_1 + 4G_1)} \quad (09)$$

$$\beta_N = \frac{-3(K_N + 2G_N)}{5G_N(3K_N + 4G_N)} \quad (10)$$

As for the bulk modulus:

$$K_{HS} = \frac{K_{HS-} + K_{HS+}}{2} \quad (11)$$

where:

$$K_{HS-} = K_1 + \frac{A_1}{1 + \alpha_1 A_1} \quad (12)$$

and

$$K_{HS+} = K_N + \frac{A_N}{1 + \alpha_N A_N} \quad (13)$$

A_1 and A_N are calculated as follows:

$$A_1 = \frac{v_N}{(K_{S_N} - K_1)^{-1} - \alpha_1} \quad (14)$$

$$A_N = \frac{v_1}{(K_{S_1} - K_N)^{-1} - \alpha_N} \quad (15)$$

$$\alpha_1 = \frac{-3}{3K_1 + 4G_1} \quad (16)$$

$$\alpha_N = \frac{-3}{3K_N + 4G_N} \quad (17)$$

Note: determine the appropriate oxide for both 1 and N are in the program, which chooses the greater value of their values (Tlili S, et al. 2017; Benatallah, N et al. 2023).

The longitudinal and transversal waves velocities are calculated from the following two relationships:

$$V_p = \sqrt{\frac{3K + 4G}{3\rho}} \quad (18)$$

and

$$V_s = \sqrt{\frac{G}{\rho}} \quad (19)$$

The bulk sound wave velocity can also be conclude from the previous two relationships as follows:

$$V_{\phi}^2 = V_p^2 - \frac{4}{3}V_s^2 \quad (20)$$

Also from the knowledge of density values and bulk modulus, this velocity can be calculated as follows:

$$V_{\phi} = \sqrt{\frac{B}{\rho}} \quad (21)$$

To calculate the difference DP between the value of the parameter $P_{(Fe_x, Ca_{(1-x)})O}$ for the compound $(Fe_x, Ca_{(1-x)})O$ and its value for the Earth's material P_{PREM} it will be according to the following relationship:

$$DP = P_{PREM} - P_{(Fe_x, Ca_{(1-x)})O} \quad (22)$$

3. RESULTS AND DISCUSSION

3.1 Compounds density

After calculation we show in (Figure 1) the change in the x-percentage values of iron soluble in calcium oxide of the formation of minerals $(Fe_x, Ca_{(1-x)})O$, where the density is close to that of the Earth's material represented in the PREM model by changing the pressures of this model from the surface to the end of the Earth's lower mantle.

Through this figure it can be observed that iron oxide density is the closest to the Earth's material in three core intervals, accounting for approximately 77.78% of the values approved from Table (1), where these intervals are as follows: the first is from the beginning of the surface up to the twenty-fourth depth, corresponding to the depth 550 km. Also, it is the case at the final limits of the Earth's upper mantle and that is at the two depths: the twenty-seventh and the following, and finally from the beginning of the thirty-ninth depth up to the end of the Earth's lower mantle. Values can be found in Table (2), which provides the values of the percentages, thousand, ten thousand and one hundred thousand for the presence of iron in the compounds $(Fe_x, Ca_{(1-x)})O$, where the density is close to its counterpart and that of the terrestrial material represented in the PREM model in the most important terrestrial layers up to the borders of the terrestrial outer core. It also provides the difference between their values and the difference between its percentage value and the rest of the ratios.

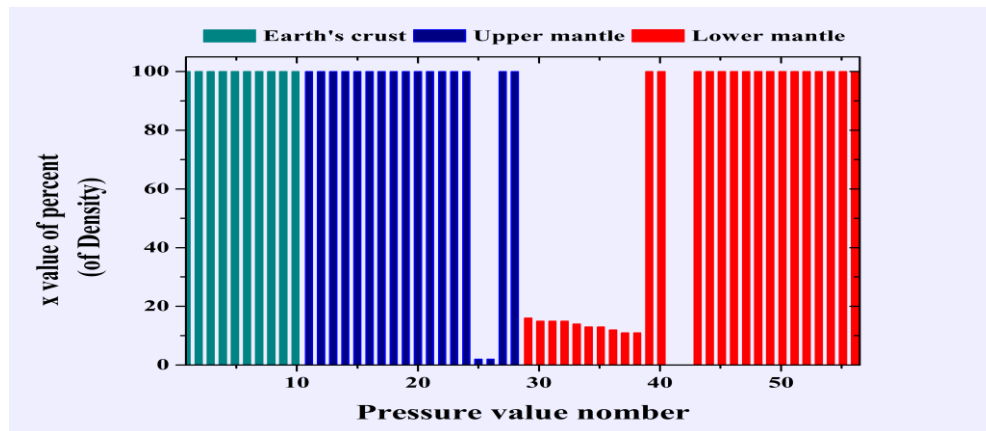


Figure 1: Shows the change in the x percentage values of Fe soluble in calcium oxide for the formation of minerals $(Fe_x, Ca_{(1-x)})O$ with near-density of the Earth's material represented in the PREM model by the change of the pressures of this model from the surface to the end of the lower Earth's mantle.

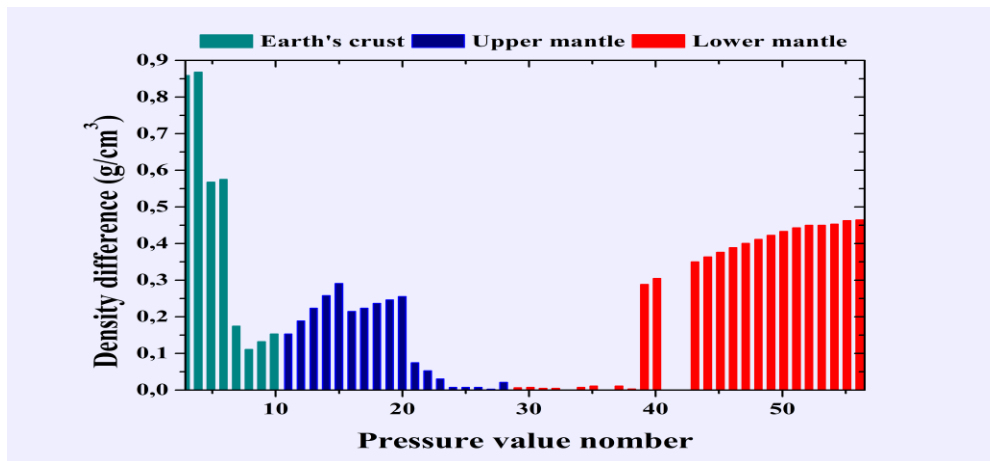


Figure 2: Shows the change in the difference in density values between the Earth’s material represented in the PREM model and those of the minerals $(Fe_x, Ca_{(1-x)})O$ with the percentage close to it by the change of the pressures of this model from the surface to the end of the lower Earth’s mantle.

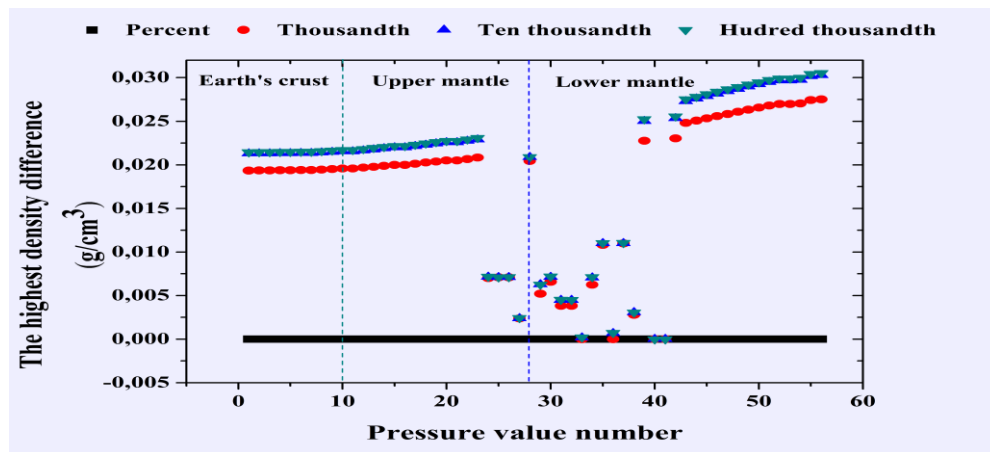


Figure 3: Shows the change in the difference the difference in density values between the Earth’s material represented in the PREM model and those of the minerals $(Fe_x, Ca_{(1-x)})O$ by a percentage, thousandth, ten thousandth and one hundred thousandth, which is close to it through the change in pressures in this model from the surface to the end of the Earth's lower mantle, taking the first difference as a reference.

Through this Table, it can also be seen that the compound at $x = 16\%$ for iron attendance appears at the beginning of the Earth's lower mantle, that is at the twenty-ninth depth. The appearance of this compound is the only one, representing approximately 1.85% of the studied depths. This same ratio is for the appearance of each of the compounds for $x = 14\%$ and $x = 12\%$ for the attendance of iron, and this is respectively at the two depths: the thirty-third and the thirty-sixth. While, the same amount it exceeds of compounds appearance percentage for $x = 2\%$, $x = 13\%$ and $x = 11\%$ for the attendance of iron, each of them appears at the two following depths, and they are respectively: the twenty-fifth and the twenty-sixth, the thirty-fourth and the thirty-fifth, the thirty-seventh and the thirty-eighth. Lastly and with the same amount it exceeds the compound's appearance percentage

for $x=15\%$, for the attendance of iron that appears between the two depths the thirtieth and the thirty-second.

Table 2: provides the values of the percentages, thousand, ten thousand and one hundred thousand for the presence of iron in the compounds $(Fe_x, Ca_{(1-x)})O$, where the density is close to its counterpart and that of the terrestrial material represented in the PREM model in the most important terrestrial layers up to the borders of the terrestrial outer core. It also provides the difference between their values and the difference between its percentage value and the rest of the ratios.

	Depth (Km)	x value of percent			
		Percent (%)	Thousandth (‰)	Ten thousandth (‱)	Hurdrend thousandth (‰‰)
Earth's Crust	0	100	1000	10000	100000
		/	/	/	/
		0	0,01935	0,02128	0,02147
	80	100	1000	10000	100000
		0,15306	0,13348	0,13153	0,13134
		0	0,01957	0,02152	0,02172
Upper Mantle	80	100	1000	10000	100000
		0,15308	0,1335	0,13155	0,13136
		0	0,01957	0,02152	0,02172
	670	100	1000	12	119
		0,0209	4,46E-04	2,70E-05	3,38E-06
		0	0,02045	0,02087	0,02089
Lower Mantle	670	16	158	1576	15760
		0,00627	0,00105	1,80E-06	1,80E-06
		0	0,00522	0,00627	0,00627
	2987	100	1000	10000	100000
		0,46469	0,43717	0,43443	0,43415
		0	0,02752	0,03027	0,03054

The iron oxide density value at the surface and the following depth directly at the depth of 3 km is very large, giving a significant difference between this value and the value available in the PREM model. Therefore, it is not represented in (Figure 2), which represents the change in the difference in density values between the Earth's material represented in the PREM model and those of the minerals $(Fe_x, Ca_{(1-x)})O$ with the percentage close to it by the change of the pressures of this model from the surface to the end of the lower Earth's mantle.

Through this figure, a vibration can be observed in the variance of this difference with more deeper into the depth where it is increasing between the two depths: the third and the fourth, the fifth and the sixth, the eighth and the fifteenth, the sixteenth and the twentieth, the twenty-seventh and the twenty-eighth, the thirty-third and the thirty-fifth and finally from the thirty-ninth to the last depth of the study. At all the highest and lowest depth are estimated respectively at 0.87 g/cm^3 and $2.13 \cdot 10^{-4} \text{ g/cm}^3$, each appearing at the two depths: the fourth of iron oxide and the thirty-third of the compound for $x = 14\%$ for the attendance of iron.

When the ratio increases from a percentage to a more accurate ratio, the compounds increase precision as the difference also increases precision. This is illustrated by Table (2) and (Figure 3), which presents the change in the difference the difference in density values between the Earth's

material represented in the PREM model and those of the minerals $(Fe_x, Ca_{(1-x)})O$ by a percentage, thousandth, ten thousandth and one hundred thousandth, which is close to it through the change in pressures in this model from the surface to the end of the Earth's lower mantle, taking the first difference as a reference.

Through the same Figure it should be noted that at the twenty-seventh depth the compound changes from iron oxide to the following compounds: for $x = 9 \text{ ‰}$, for $x = 90 \text{ ‰}$ and for $x = 897 \text{ ‰}$. The compound also changes from iron oxide to the following two compounds: for $x = 12 \text{ ‰}$ and for $x = 119 \text{ ‰}$ at the twenty-seventh depth. It can also be seen that the decrease in the difference is increasing with the increase in depth, this increase is very slow from the depth of the surface up to the twenty-third depth, while it is faster between the two depths: the thirty-ninth and the last depth and between the two regions there is a clear vibration. Also, the amount of the lower difference changes to $5.64 \cdot 10^{-7} \text{ g/cm}^3$, and the compound also changes which appears for it, it is the compound with the ratio $x = 1699 \text{ ‰}$ for the attendance of iron and this is at the exact twenty-sixth depth.

3.2 Elastic modulus of compounds

Through (Figure 4), the shear modulus of the compound for $x = 3\%$ for the attendance of iron it is closest to its value in PREM model from the surface up to the twenty-fourth depth, with the estimated appearance ratio of 44.44% of the studied depths. But starting from the following depth up to the end of the upper mantle, that is at the twenty-eighth depth, the compound appears for $x = 17\%$ for the attendance of iron, this is 7.41% from those studied depths. Moreover, by a quarter of this ratio the following compounds appear for $x = 82\%$, $x = 91\%$ and $x = 99\%$, which appear respectively at the depths; the twenty-ninth, the following depth and the thirty-third. In addition, by half that ratio and at the two following depths starting at the thirty-first depth, the compound appears for $x = 98\%$. Finally, iron oxide appears at 38.89%, from the thirty-fourth up to the last depth on the limits of the Earth's outer core. All of this results from the calculation recorded for some of its results in Table (3) and also the representative in (Figure 4), which shows the change in the x percentage values of Fe soluble in calcium oxide of minerals $(Fe_x, Ca_{(1-x)})O$ with a shear modulus close to that of the Earth's material represented in the PREM model by the change of the pressures of this model from the surface to the end of the lower Earth's mantle

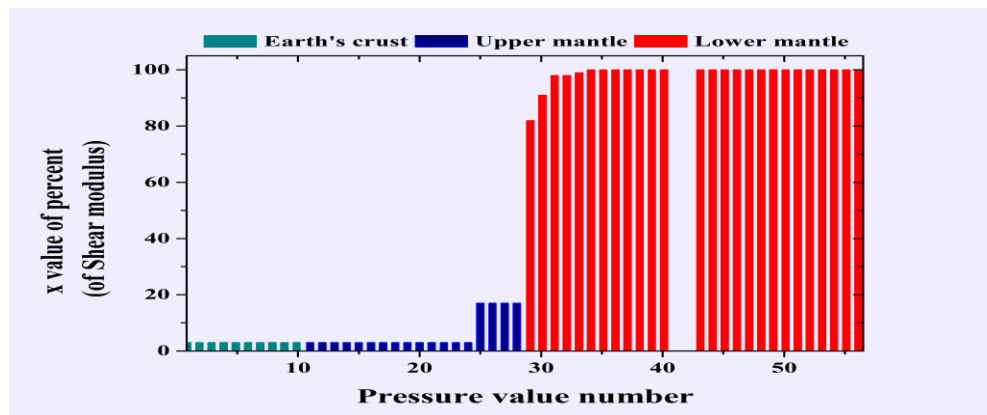


Figure 4: shows the change in the x percentage values of Fe soluble in calcium oxide of minerals $(Fe_x, Ca_{(1-x)})O$ with a shear modulus close to that of the Earth's material represented in the PREM model by the change of the pressures of this model from the surface to the end of the lower Earth's mantle.

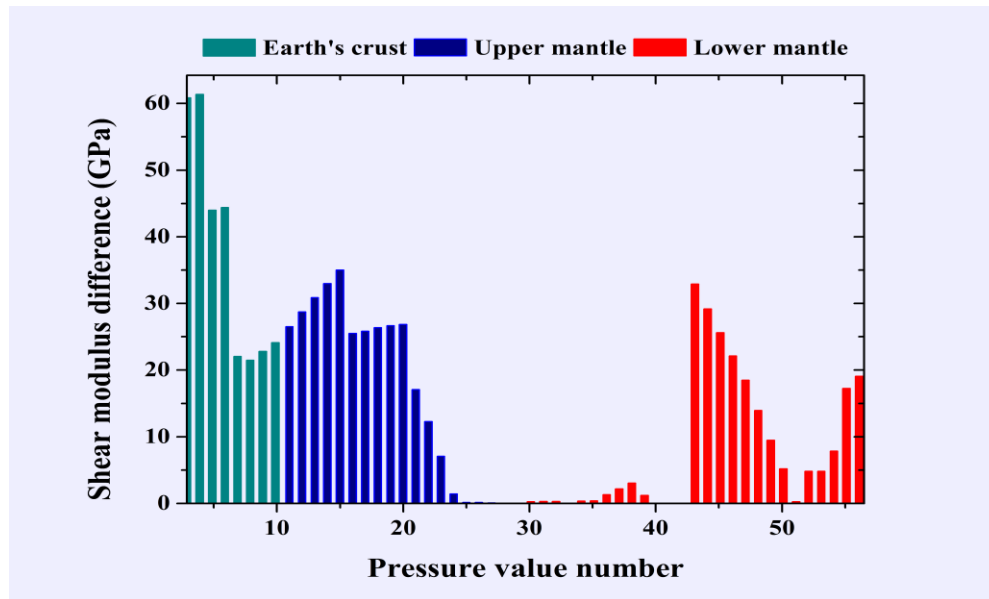


Figure 5: shows variance of the difference in the shear modulus values between the Earth's material represented in the PREM model and those of the minerals $(Fe_x, Ca_{(1-x)})O$ by change of the pressures of this model from the surface to the end of the lower Earth's mantle.

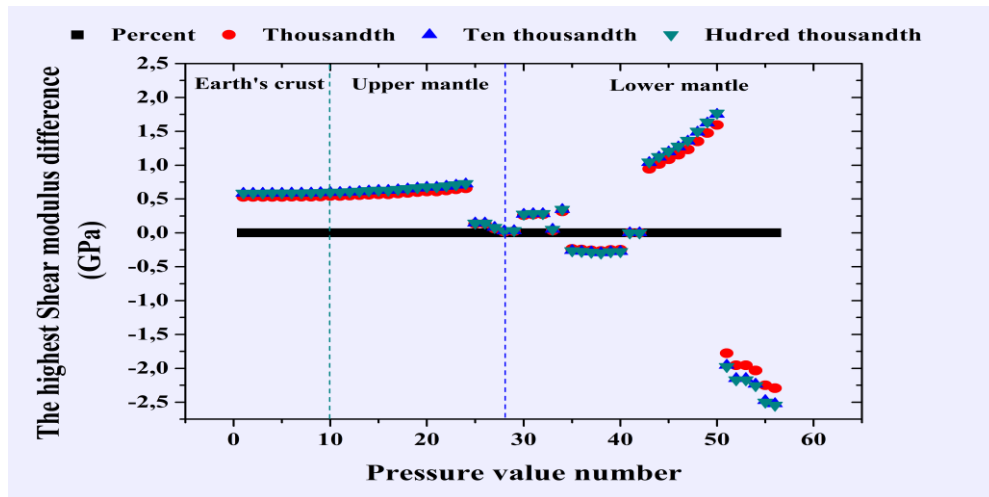


Figure 6: shows the change in the difference the difference in shear modulus values between the Earth's material represented in the PREM model and those of the minerals $(Fe_x, Ca_{(1-x)})O$ by a percentage, thousandth, ten thousandth and one hundred thousandth, which is close to it through the change in pressures in this model from the surface to the end of the Earth's lower mantle, taking the first difference as a reference.

Table 3: provides the values of the percentages, thousand, ten thousand and one hundred thousand for the presence of iron in the compounds $(Fe_x, Ca_{(1-x)})O$, where the shear modulus is close to its

counterpart and that of the terrestrial material represented in the PREM model in the most important terrestrial layers up to the borders of the terrestrial outer core. It also provides the difference between their values and the difference between its percentage value and the rest of the ratios.

	Depth (Km)	x value of percent			
		Percent (%)	Thousandth (‰)	Ten thousandth (‱)	Hundredth thousandth (‰‰)
Earth's Crust	0	3	3	3	3
		/	/	/	/
		0	0,53122	0,58317	0,58836
	80	3	3	3	3
		24,10517	23,56224	23,50914	23,50384
		0	0,54293	0,59603	0,60133
Upper Mantle	80	3	3	3	3
		26,50165	25,95871	25,90561	25,90031
		0	0,54294	0,59604	0,60134
	670	17	167	1662	16619
		0,02971	0,01305	9,95E-04	1,64E-04
		0	0,01665	0,02871	0,02954
Lower Mantle	670	82	822	8220	82201
		0,03338	0,00939	4,39E-04	2,03E-04
		0	0,02399	0,03294	0,03318
	2987	100	1000	10000	100000
		19,08239	21,37506	21,60445	21,62739
		0	-2,29267	-2,52205	-2,54499

Only in specific intervals does the value of the difference in the shear modulus between the earth material represented in the PREM model and that of the minerals $(Fe_xCa_{1-x})O$ with a percentage close to it increase, which also fluctuates and is represented by its change with the change in pressures of this model from the surface to the end of the lower mantle in (Figure 5). After the exception of the same first two depths and for the same reason always, these domains are compatible with density up to the twentieth depth as previously. In addition to the following domains: between the two depths the third and the fourth, between the fifth and the sixth, the eighth and the fifteenth, the sixteenth and the twentieth, between the twenty-eighth and the thirty-second, between the thirty-third and the thirty-eighth, between the fortieth and the following depth and finally between the forty-ninth and the last depth. At all the highest and lowest depth are estimated respectively at 87.32 and $2.40 \cdot 10^{-2} \text{GPa}$, each appearing at the two depths: the fourth as it was for the density and the fortieth for the following two compounds, compound for $x = 3\%$ for the attendance of iron and iron oxide.

When the ratio increases from a percentage to a more accurate ratio, the compounds increase precision. The most change is at the thirty-fourth depth, the apparent iron oxide is transformed into another compound very close to it, the following compounds; for $x = 999 \text{‰}$, for $x = 9989 \text{‱}$ and for $x = 99894 \text{‰‰}$. But the most obvious is the small difference with that increase in compounds accuracy, as noticing from (Figure 6) and the values of Table (4) that the difference is slowly decreasing as depth increases up to the twenty-fourth depth, more slowly between the two depths: the thirtieth and the thirty-second, and much faster decrease in the two domains; between the thirty-

third and the next and between the forty-first and the forty-eighth, while between the two depths: the twenty-fourth and the thirtieth, the decrease in the difference is decreasing with the increase of the depth. However, there is an increase in this difference in two domains, a slowing increase between the thirty-fifth and the fortieth depth, while faster from the forty-ninth depth up to the limits of the Earth's outer core.

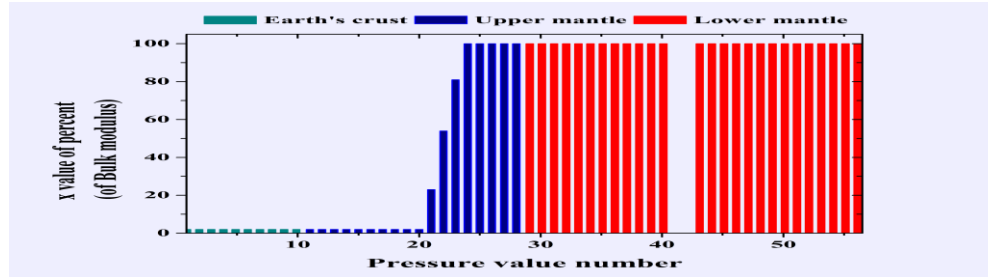


Figure 7: shows the change in the x percentage values of Fe soluble in calcium oxide of minerals $(Fe_x, Ca_{(1-x)})O$ with a bulk modulus close to that of the Earth's material represented in the PREM model by the change of the pressures of this model from the surface to the end of the lower Earth's mantle.

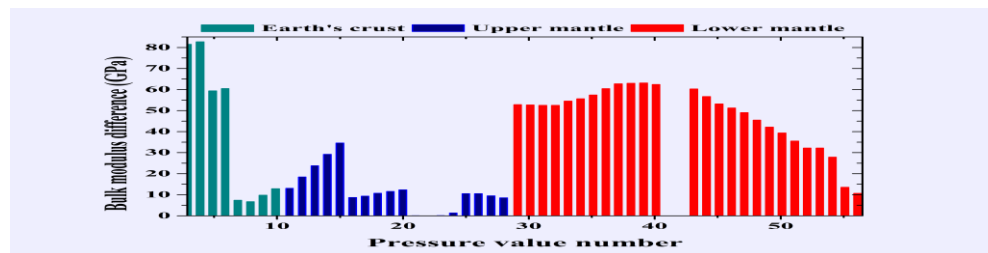


Figure 8: shows variance of the difference in the bulk modulus values between the Earth's material represented in the PREM model and those of the minerals $(Fe_x, Ca_{(1-x)})O$ by change of the pressures of this model from the surface to the end of the lower Earth's mantle.

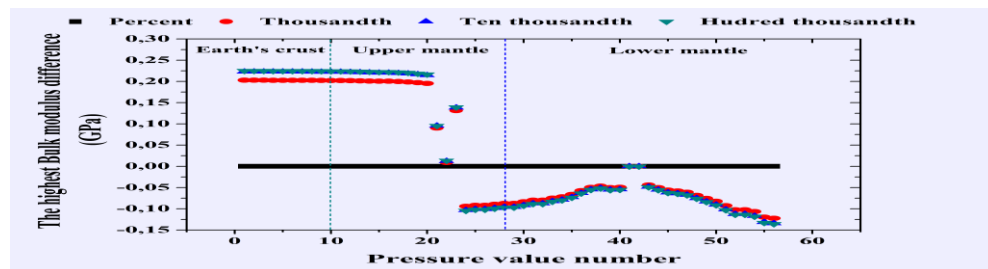


Figure 9: shows the change in the difference the difference in bulk modulus values between the Earth's material represented in the PREM model and those of the minerals $(Fe_x, Ca_{(1-x)})O$ by a percentage, thousandth, ten thousandth and one hundred thousandth, which is close to it through the change in pressures in this model from the surface to the end of the Earth's lower mantle, taking the first difference as a reference.

(Figure 6) presents the change in the difference the difference in shear modulus values between the Earth's material represented in the PREM model and those of the minerals $(Fe_x, Ca_{(1-x)})O$ by a

percentage, thousandth, ten thousandth and one hundred thousandth, which is close to it through the change in pressures in this model from the surface to the end of the Earth's lower mantle, taking the first difference as a reference. It also shows that the amount of the lower difference changes, reaching $1.86 \cdot 10^{-5} GPa$, and the compound changes also which appears for it so that the compound is $x = 16126 \text{ ‰}$ for the attendance of iron and this is at the twenty-fifth depth exactly.

From (Figure 7) it is clear that the bulk modulus of the compound for $x = 2\%$ for the attendance of iron is the closest to those of its especial values in PREM model starting from the surface up to the twentieth depth, with an estimated appearance of 37.04% of the studied depths. It also shows iron oxide at 57.41%, starting from the thirty-fourth depth up to the last depth on the limits of the Earth's outer core. Between the appearance of the two mentioned compounds previously and at each of the three depths, each of the compounds appear respectively for $x = 23\%$, $x = 54\%$ and $x = 81\%$, this is 1.85% of those studied depths. These results came after calculation and are partially recorded in Table (4) and also represented in (Figure 7), which shows the change in the x percentage values of Fe soluble in calcium oxide of minerals $(Fe_x, Ca_{(1-x)})O$ with a bulk modulus close to that of the Earth's material represented in the PREM model by the change of the pressures of this model from the surface to the end of the lower Earth's mantle.

With the same previous exception and for the same reason, it is not represented in (Figure 8), which represents variance of the difference in the bulk modulus values between the Earth's material represented in the PREM model and those of the minerals $(Fe_x, Ca_{(1-x)})O$ by change of the pressures of this model from the surface to the end of the lower Earth's mantle. Through this figure, we can observe the permanent vibration in the change of this difference, as it is increasing before the twentieth depth in the same domains of the density and the shear modulus. Adding to the following domains: between the two depths: the twenty-second and twenty-fifth, between the twenty-eighth and the following, and finally between the thirty-first and the thirty-ninth. At all the highest and lowest depth are estimated respectively at 82.77 and $1.33 \cdot 10^{-2} GPa$, with the first appearing at the same depth as the fourth as well and the second appearing at the twenty-second depth for the following two compounds, the compound for $x = 2\%$ and for $x = 54\%$ for the attendance of iron.

Table 4: provides the values of the percentages, thousand, ten thousand and one hundred thousand for the presence of iron in the compounds $(Fe_x, Ca_{(1-x)})O$, where the bulk modulus is close to its counterpart and that of the terrestrial material represented in the PREM model in the most important terrestrial layers up to the borders of the terrestrial outer core. It also provides the difference between their values and the difference between its percentage value and the rest of the ratios.

	Depth (Km)	x value of percent			
		Percent (%)	Thousandth (‰)	Tenthousandth (‱)	Hurdrendthousandth (‰‰)
Earth's crust	0	2	2	2	2
		0	0,20281	0,22293	0,22494
	80	2	2	2	2
		12,93371	12,73152	12,71145	12,70945
		0	0,20219	0,22225	0,22426
Upper mantle	80	2	2	2	2
		13,13085	12,92866	12,90859	12,90659
		0	0,20219	0,22225	0,22426
	670	100	1000	10000	100000
		8,57502	8,66228	8,67095	8,67181

Lowermantle		0	-0,08726	-0,09593	-0,09679
	670	100	1000	10000	100000
		52,90781	52,99507	53,00373	53,0046
		0	-0,08726	-0,09593	-0,09679
	2987	100	1000	10000	100000
		10,75935	10,88175	10,89392	10,89514
		0	-0,1224	-0,13458	-0,13579

The same case, for this parameter, when the ratio increases from a percentage to a more accurate ratio the compounds increase in precision and the difference decreasing starting from the surface to the twenty-third depth. This decrease is very slowly down to the twentieth depth, and from this depth to the twenty-second depth, the decrease is faster. Finally, this is increasing significantly, from the last depth to the following depth. However, from the twenty-fourth to end depth, the difference is increasing. This increase is changing as the depth increases somewhat slowly, fixely and increasingly faster than before in the following domains: starting from the depth of its appearance to the thirty-sixth depth, from the following depth to the fortieth depth and finally from the following depth up to the last depth at the limits of the earth’s outer core. This is evident from Table (4) and (Figure 9), which represents the change in the difference the difference in bulk modulus values between the Earth’s material represented in the PREM model and those of the minerals $(Fe_x, Ca_{(1-x)})O$ by a percentage, thousandth, ten thousandth and one hundred thousandth, which is close to it through the change in pressures in this model from the surface to the end of the Earth's lower mantle, taking the first difference as a reference. Also, the amount of the lower difference changes to $3.52 \cdot 10^{-6} GPa$, and the compound changes too which appears for it, so that the compound is $x = 80799 \text{ ‰}$ for the attendance of iron and this is at the twenty-third depth exactly

3.3 Elastic wave velocity of compounds

Our calculations also produce both Figures (10-18) and Table (5-7) where:

Table (5, 6 and 7): which records the values of different ratios of iron attendance in $(Fe_x, Ca_{(1-x)})O$ compounds and the difference in the waves velocities of longitudinal and transversal, bulk sound between these compounds and between the Earth's material which represented their values in PREM model in the Earth’s most important limits.

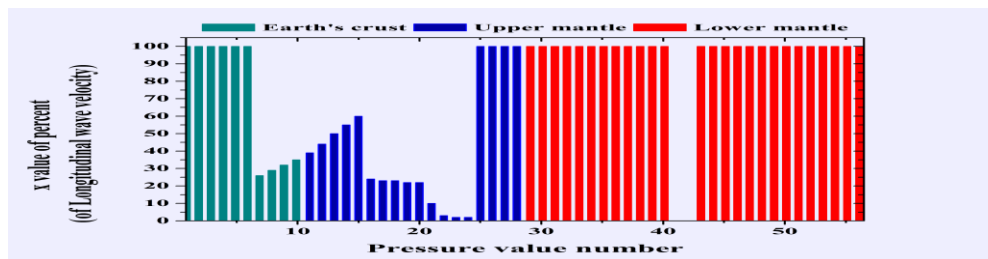


Figure 10: shows the change in x percentage values of Fe soluble in calcium oxide of the formation of minerals $(Fe_x, Ca_{(1-x)})O$ with a longitudinal wave velocity close to that of the Earth’s material represented in the PREM model by the change of the pressures of this model from the surface to the end of the lower Earth’s mantle.

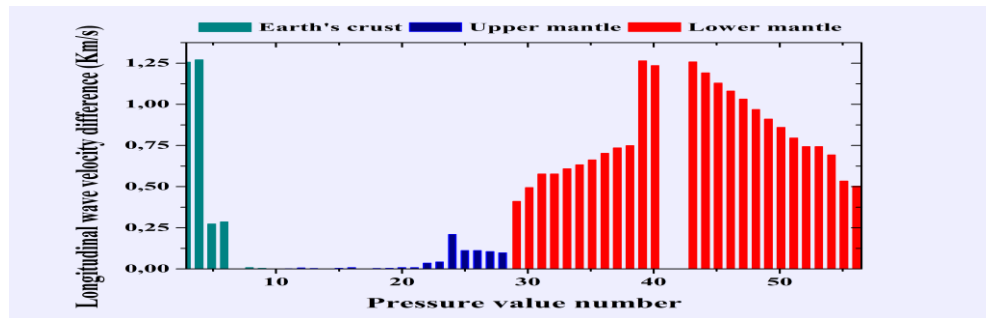


Figure 11: shows variance in longitudinal wave velocity values between the Earth’s material represented in the PREM model and those of the $(Fe_x, Ca_{(1-x)})O$ with a percentage close to it by the change of the pressures of this model from the surface to the end of the lower Earth’s mantle.

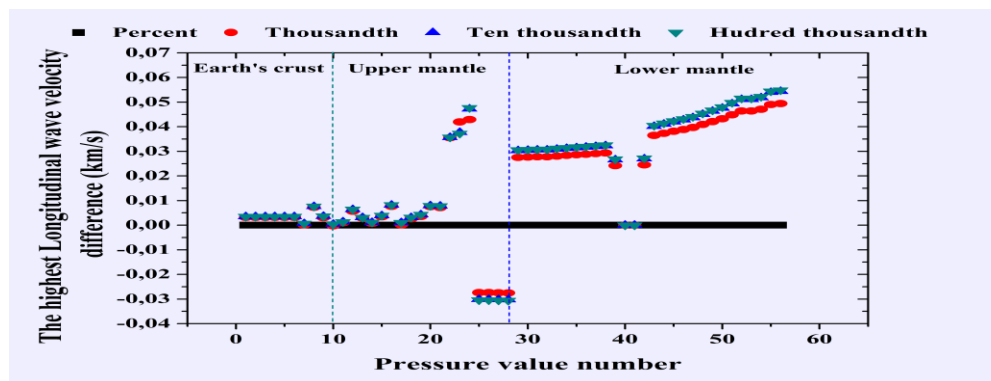


Figure 12: shows the change in the difference the difference in longitudinal wave velocity values between the Earth’s material represented in the PREM model and those of the minerals $(Fe_x, Ca_{(1-x)})O$ by a percentage, thousandth, ten thousandth and one hundred thousandth, which is close to it through the change in pressures in this model from the surface to the end of the Earth’s lower mantle, taking the first difference as a reference.

Figure (10): represents the change in x percentage values of Fe soluble in calcium oxide of the formation of minerals $(Fe_x, Ca_{(1-x)})O$ with a longitudinal wave velocity close to that of the Earth’s material represented in the PREM model by the change of the pressures of this model from the surface to the end of the lower Earth’s mantle.

According to them, iron oxide longitudinal wave velocity values are closer to those special Earth's material approximately of 66.67% from those studied depths. This is from the surface to the sixth depth and from the twenty-fifth to the last studied depth, that is, this apperance is in the first quarter of the Earth's crust and just below the beginning of the Earth's lower mantle. This velocity is also for the following compounds for x = 26%, x = 29%, x = 32%, x = 35%, x = 39%, x = 44%, x = 50%, x = 55%, x = 60% and x = 24% is the closest starting from the seventh depth to the sixteenth depth respectively, as well as for x = 10% and x = 3% is the closest starting from the twenty-first and the following depth. The ratio of its attendance from the studied depths is close to 1.85%. This ratio doubles for the two compounds for x = 23%, x = 22% and x = 2%, which appear respectively at the four following depths: starting from the seventeenth and the two following depths starting from the twenty-third depth.

(Figure 11): represents variance in longitudinal wave velocity values between the Earth’s material represented in the PREM model and those of the $(Fe_x, Ca_{(1-x)})O$ with a percentage close to it by the change of the pressures of this model from the surface to the end of the lower Earth’s mantle.

The two values of the difference are not represented by the same two depths mentioned earlier in this figure, this is also for the same reason. Through this figure, we can observe the permanent vibration in the change of this difference, as it is increasing with the same increase of previous parameters up to the sixth depth. Adding to the following domains, between the seventh and the eighth, the tenth and the twelfth, the fourteenth and the sixteenth, the seventeenth and the twentieth, the twenty-first and the twenty-sixth, the twenty-eighth and the thirty-ninth, and finally between the fortieth and the following depth. Where the highest and lowest depth ever is estimated respectively 1.27 and $7.7 \cdot 10^{-4}$ km/s, the second appears at the seventh depth, and the first is always at the fourth depth, and this is for the following two compounds, iron oxide and the compound for $x = 26\%$ for the attendance of iron.

Table 5: provides the values of the percentages, thousand, ten thousand and one hundred thousand for the presence of iron in the compounds $(Fe_x, Ca_{(1-x)})O$, where the longitudinal wave velocity is close to its counterpart and that of the terrestrial material represented in the PREM model in the most important terrestrial layers up to the borders of the terrestrial outer core. It also provides the difference between their values and the difference between its percentage value and the rest of the ratios.

	Depth (Km)	x value of percent			
		Percent (%)	Thousandth (‰)	Ten thousandth (‱)	Hurdrend thousandth (‱‱)
Earth's Crust	0	100	1000	10000	100000
		/	/	/	/
		0	0,00319	0,00351	0,00354
	80	35	350	3505	35054
		4,74E-04	7,39E-04	5,66E-05	4,30E-06
		0	-2,66E-04	4,17E-04	4,69E-04
Upper Mantle	80	39	390	3898	38979
		0,0014	4,32E-04	2,10E-05	4,40E-06
		0	9,65E-04	0,00138	0,00139
	670	100	1000	10000	100000
		0,09797	0,12551	0,12827	0,12854
		0	-0,02754	-0,0303	-0,03058
Lower Mantle	670	100	1000	10000	100000
		0,41092	0,38337	0,38062	0,38034
		0	0,02754	0,0303	0,03058
	2987	100	1000	10000	100000
		0,50344	0,454	0,44905	0,44855
		0	0,04944	0,05439	0,05488

(Figure 12): represents the change in the difference the difference in longitudinal wave velocity values between the Earth’s material represented in the PREM model and those of the minerals $(Fe_x, Ca_{(1-x)})O$ by a percentage, thousandth, ten thousandth and one hundred thousandth, which is close to it through the change in pressures in this model from the surface to the end of the Earth's lower mantle, taking the first difference as a reference.

Also when the ratio increases from a percentage to a more accurate ratio, the compounds increase precision. Through (Figure 12) and Table (5) it can be seen that the most obvious change is the increase in the difference with that increase in the accuracy of the compounds, which means that this accuracy is not helpful, and this is only at the four following depths starting from the twenty-fifth depth where this increase is constant at all depths. While from the surface to the sixth depth, the decrease of difference with increased precision in compounds is constant, his decrease increases with increasing depth penetration in the following intervals: between the two depths: the seventh and the eighth, the tenth and the twelfth, the fifteenth and the following, the seventeenth and the twentieth, the twenty-first and the twenty-fourth, the twenty-ninth and the thirty-eighth, and finally from the thirty-ninth depth up to the limits of the Earth's outer core. It also appears that the amount of the lower difference changes which reaching $1.31 \cdot 10^{-5}$ km/s and the compound changes too which appears for it, so that the compound is $x = 31869\%$ for the attendance of iron and this is at the ninth depth exactly.

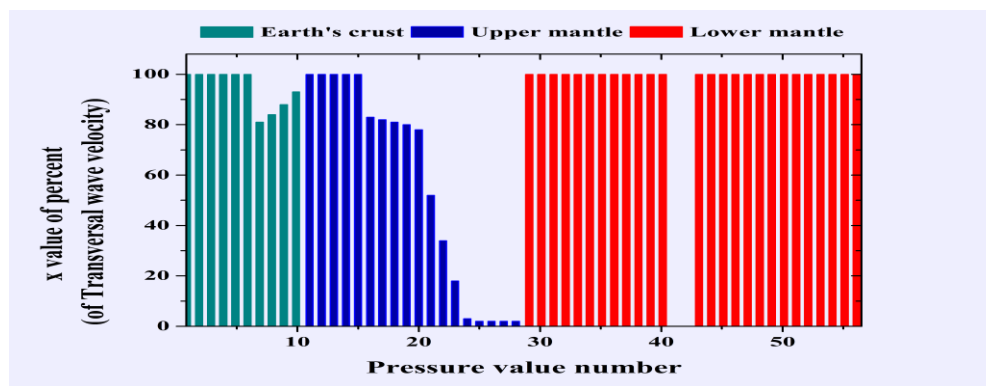


Figure 13: shows the change in x percentage values of Fe soluble in calcium oxide of the formation of minerals $(Fe_x, Ca_{(1-x)})O$ with transversal wave velocity close to that of the Earth's material represented in the PREM model by the change of the pressures of this model from the surface to the end of the lower Earth's mantle.

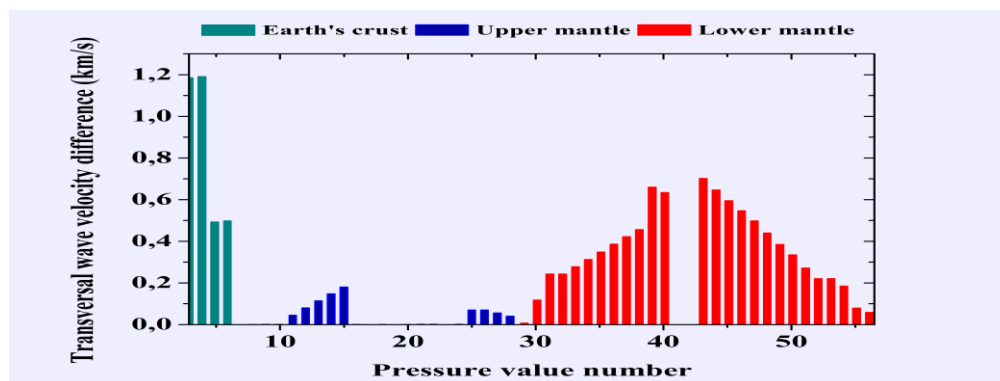


Figure 14: shows variance in the transversal wave velocity values between the Earth's material represented in the PREM model and those of the $(Fe_x, Ca_{(1-x)})O$ with percentage close to it by the change of the pressures of this model from the surface to the end of the lower Earth's mantle.

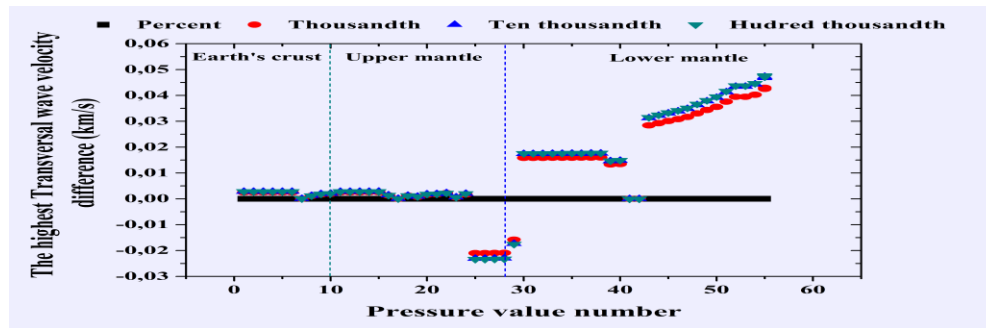


Figure 15: shows the change in the difference the difference in transversal wave velocity values between the Earth's material represented in the PREM model and those of the minerals $(Fe_x, Ca_{(1-x)})O$ by a percentage, thousandth, ten thousandth and one hundred thousandth, which is close to it through the change in pressures in this model from the surface to the end of the Earth's lower mantle, taking the first difference as a reference.

Figure (13): represents the change in x percentage values of Fe soluble in calcium oxide of the formation of minerals $(Fe_x, Ca_{(1-x)})O$ with transversal wave velocity close to that of the Earth's material represented in the PREM model by the change of the pressures of this model from the surface to the end of the lower Earth's mantle.

In addition to this Figure and Table (6), it can be seen that the values of this velocity which special for iron oxide are closer to those special of the Earth's material by a depth increase over the previous velocity, which increases the ratio of those studied depths by 1.85%. Where that is in three domains, the first is the same first quarter of the Earth's crust, which had longitudinal wave velocity. The second is from the eleventh depth to the fifteenth depth and finally at all the Earth's lower mantle, starting from the twenty-ninth up to the last studied depth. The increase in the above ratio represents the same amount of appearance as the following compounds for $x = 81\%$, $x = 84\%$, $x = 88\%$, $x = 93\%$, $x = 83\%$, $x = 82\%$, $x = 81\%$, $x = 80\%$, $x = 78\%$, $x = 52\%$, $x = 34\%$, $x = 18\%$ and $x = 3\%$, which consider the closest in the two domains. The first four compounds appear at the following fourth depths starting from the twelfth depth respectively, while the rest of the compounds appear at the ninth following depths from the sixteenth depth. Finally, in the four following depths to this depth, the compound appears for $x = 2\%$ for the attendance of iron, by the ratio four times of the previous ratio.

(Figure 14): represents variance in the transversal wave velocity values between the Earth's material represented in the PREM model and those of the $(Fe_x, Ca_{(1-x)})O$ with percentage close to it by the change of the pressures of this model from the surface to the end of the lower Earth's mantle.

Through this figure the highest and the lowest depth ever estimated respectively at 1.19 km/s and $8.17 \cdot 10^{-5}$ km/s, the latter appears at the seventeenth depth for the compound for $x = 82\%$ for the attendance of iron. While the first always appears at the fourth depth, this is for iron oxide. Also for the same reason, in this figure, the two difference values are not represented the same two depths as previously mentioned. Through this figure, we can observe the permanent vibration in the change of this difference, where it is increasing in the same domains of longitudinal wave velocity increased, except in the following domains; between the two depths: the seventh and the fifteenth, the seventeenth and the following, the nineteenth and the twenty-second, the twenty-third and the twenty-fifth, the thirtieth and the thirty-ninth.

Table 6: provides the values of the percentages, thousand, ten thousand and one hundred thousand for the presence of iron in the compounds $(Fe_x, Ca_{(1-x)})O$, where the transversal wave velocity is close to its counterpart and that of the terrestrial material represented in the PREM model in the most important terrestrial layers up to the borders of the terrestrial outer core. It also provides the difference between their values and the difference between its percentage value and the rest of the ratios.

	Depth (Km)	x value of percent			
		Percent (%)	Thousandth (‰)	Ten thousandth (‱)	Hundred thousandth (‱‱)
Earth's Crust	0	100	1000	10000	100000
		/	/	/	/
		0	0,00255	0,0028	0,00283
	80	93	922	9212	92114
		0,00208	2,07E-04	1,03E-05	3,28E-07
		0	0,00188	0,00207	0,00208
Upper Mantle	80	100	1000	10000	100000
		0,04588	0,04333	0,04308	0,04305
		0	0,00255	0,0028	0,00283
	670	2	2	2	2
		0,04115	0,06206	0,06415	0,06436
		0	-0,02091	-0,02301	-0,02322
Lower Mantle	670	100	1000	10000	100000
		0,00755	0,02336	0,02494	0,0251
		0	-0,01581	-0,01739	-0,01755
	2987	100	1000	10000	100000
		0,05965	0,01671	0,01241	0,01198
		0	0,04294	0,04724	0,04767

(Figure 15): represents the change in the difference the difference in transversal wave velocity values between the Earth's material represented in the PREM model and those of the minerals $(Fe_x, Ca_{(1-x)})O$ by a percentage, thousandth, ten thousandth and one hundred thousandth, which is close to it through the change in pressures in this model from the surface to the end of the Earth's lower mantle, taking the first difference as a reference.

There is an increase in the accuracy of the iron ratio in compounds, which appears when the ratio increases from a percentage to a more accurate ratio. From Table (6) and (Figure 15), it can be noted that the difference is consistent decreasing as depth changes for the following domains, The same first domain for the constant difference in the longitudinal wave velocity, between the two depths: the eleventh and the fifteenth, the twentieth and the following, and finally between the two depths the thirtieth and the fortieth. While this difference is decreasing increasingly between the two depths: the seventh and the tenth, the seventeenth and the following, the nineteenth and the following, the twenty-third and the following, and finally from the thirty-eighth depth up to limits of the Earth's outer core. There is also agreement with what came for the velocity of the previous wave in the domain of increasing the fixed unhelpful difference in depth change, in addition to the decrease in the increase of this difference between the twenty-eighth and the following depth. There is also a change in the positioning of the lower difference, its value and the compound which for it, which it is at the twentieth depth and its value is $2.91 \cdot 10^{-7} \text{ km/s}$ and the compound for $x = 78122 \text{ ‰}$.

(Figure 16): represents the change in x percentage values of Fe soluble in calcium oxide of the formation of minerals $(Fe_x, Ca_{(1-x)})O$ with bulk sound wave velocity close to that of the Earth's material represented in the PREM model by the change in the pressures of this model from the surface to the end of the lower Earth's mantle.

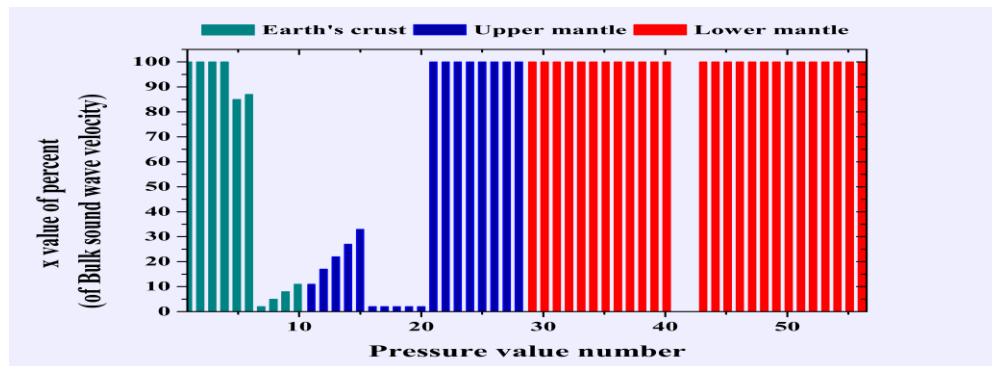


Figure 16: shows the change in x percentage values of Fe soluble in calcium oxide of the formation of minerals $(Fe_x, Ca_{(1-x)})O$ with bulk sound wave velocity close to that of the Earth's material represented in the PREM model by the change in the pressures of this model from the surface to the end of the lower Earth's mantle.

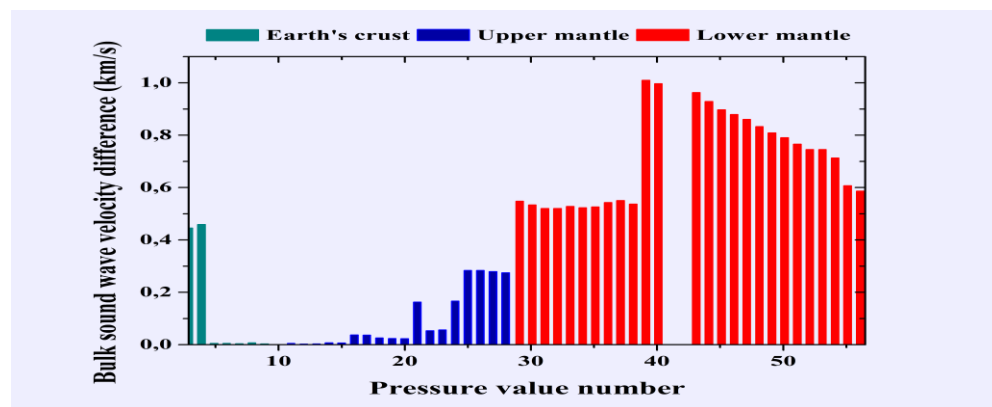


Figure 17: shows variance of the difference in bulk sound wave velocity values between the Earth's material represented in the PREM model and those of $(Fe_x, Ca_{(1-x)})O$ with a percentage close to it, by the change of the pressures of this model from the surface to the end of the lower Earth's mantle.

Through this figure and Table (7) it can also be observed that the values of this velocity which special of iron oxide are closer to those special of the Earth's material by increasing the depth over the previous velocity, by the same special ratio of the transversal wave velocity from those studied depths. But with slight differences, where is the appearance of that in only two domains. The first is less than one eighth (1/8) of the Earth's crust which ending at the fourth depth, which naturally starts from the surface. The second starts from about the middle of the upper mantle and exactly from the fourth depth, and ends on the end of the Earth's lower mantle. In the fourth depth and between the two depths the sixteenth and the twentieth, the compound appears for $x = 2\%$ of iron attendance ratio, by a ratio estimated at 11.11% of those studied depths. One third (1/3) of this ratio is the strength of the compound's attendance for $x = 11\%$ of iron attendance ratio, which appears at the two following depth starting from the tenth depth. As for one sixth (1/6) of this ratio is the

appearance ratio of the following compounds for $x = 85\%$, $x = 87\%$, $x = 5\%$, $x = 8\%$, $x = 83\%$, $x = 17\%$, $x = 22\%$, $x = 27\%$ and $x = 33\%$, which are the closest in three different domains. The first two compounds appear at the following depths from the fifth depth, the two following compounds also appear at the following depths from the eighth depth, and finally the remaining compounds appear from the twelfth depth to the fifteenth depth.

(Figure 17): represents variance of the difference in bulk sound wave velocity values between the Earth's material represented in the PREM model and those of $(Fe_x, Ca_{(1-x)})O$ with a percentage close to it, by the change of the pressures of this model from the surface to the end of the lower Earth's mantle.

Through this figure, the highest difference is for the same oxide and at the same depth for the velocity of the previous wave, which is estimated at 0.46 km/s . While the lowest is estimated at $6.04 \cdot 10^{-4} \text{ km/s}$, and the apparent for the compound for $x = 11\%$ for the attendance of iron at the tenth depth. Also, through this figure, we can observe that permanent vibration in the change of this difference, as it is increasing in the same domains of the longitudinal wave velocity increase, except in the following domains; between the two depths the tenth and the following, the twelfth and the fourteenth, the fifteenth and the following, the twentieth and the following, the twenty-second and the twenty-fifth, the twenty-eighth and the following, the thirty-second and the following, the thirty-fourth and the thirty-seventh, and finally the thirty-eighth and the following.

(Figure 18): represents the change in the difference the difference in bulk sound wave velocity values between the Earth's material represented in the PREM model and those of the minerals $(Fe_x, Ca_{(1-x)})O$ by a percentage, thousandth, ten thousandth and one hundred thousandth, which is close to it through the change in pressures in this model from the surface to the end of the Earth's lower mantle, taking the first difference as a reference.

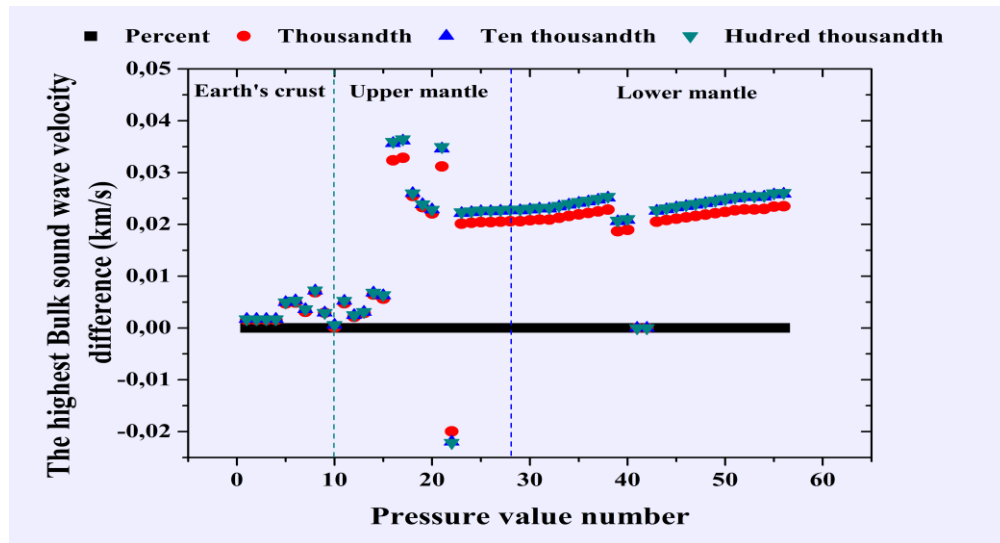


Figure 18: shows the change in the difference the difference in bulk sound wave velocity values between the Earth's material represented in the PREM model and those of the minerals $(Fe_x, Ca_{(1-x)})O$ by a percentage, thousandth, ten thousandth and one hundred thousandth, which is close to it through the change in pressures in this model from the surface to the end of the Earth's lower mantle, taking the first difference as a reference.

Table 7: provides the values of the percentages, thousand, ten thousand and one hundred thousand for the presence of iron in the compounds $(Fe_x, Ca_{(1-x)})O$, where the bulk sound wave velocity is close to its counterpart and that of the terrestrial material represented in the PREM model in the most important terrestrial layers up to the borders of the terrestrial outer core. It also provides the difference between their values and the difference between its percentage value and the rest of the ratios.

	Depth (Km)	x value of percent			
		Percent (%)	Thousandth (‰)	Ten thousandth (‱)	Hundred thousandth (‱‱)
Earth's Crust	0	100	1000	10000	100000
		/	/	/	/
		0	0,00155	0,0017	0,00172
	80	11	110	1103	11029
		6,04E-04	4,62E-04	1,34E-05	5,53E-07
		0	1,41E-04	5,90E-04	6,03E-04
Upper Mantle	80	11	113	1133	11333
		0,00528	5,26E-04	5,06E-05	2,97E-06
		0	0,00476	0,00523	0,00528
	670	100	1000	10000	100000
		0,27498	0,25435	0,25229	0,25208
		0	0,02063	0,02269	0,0229
Lower Mantle	670	100	1000	10000	100000
		0,54789	0,52726	0,5252	0,52499
		0	0,02063	0,02269	0,0229
	2987	100	1000	10000	100000
		0,58645	0,56295	0,5606	0,56036
		0	0,0235	0,02586	0,02609

When increasing the accuracy of the iron ratio in compounds from a percentage to ratio more accurate, according to Table (7) and (Figure18) it can be observed that the difference is always decreasing regardless of depth except for the twenty-second depth. This decrease is consistent as depth changes, thus it is similar to the first four depths for the difference of the two previous waves velocities. In addition to the following domains between the two depths: the twenty-fifth and the following, the twenty-eighth and the following, the thirty-first and the following, and finally, the fiftieth and the following. While the increase in this difference is for the following domains: between the two depths the fourth and sixth, the seventh and the following, the tenth and the following, the twelfth and the following, the fifteenth and the seventeenth, the twentieth and the twenty-first, the twenty-third and the twenty-fifth, the twenty-sixth and the twenty-eighth, the twenty-ninth and the thirty-first, the thirty-second and the thirty-eighth, the thirty-ninth and the fiftieth and finally from the fifty-first depth to the last studied depth. Also, everything related to the lower difference changes clearly, where it is at the tenth depth, which its value is $5.53 \cdot 10^{-7}$ km/s for the compound for $x = 11029 \text{ ‱‱}$.

4. CONCLUSION

Through calculations based on the relationship between metallurgy and seismology on the one hand, and Hashin & Shtrikman relationships on the other. We were able to get:

1. The values of the density, bulk and shear modulus, longitudinal and transverse and bulk sound wave velocities of the compounds $(Fe_x, Ca_{(1-x)})O$ are close to those of the Earth's material up to the outer core.
2. Obtaining the values of those studied parameters, especially at the most important limits between the Earth's internal layers.
3. Approximate agreement in the values of the three waves velocities, especially in the presence of iron oxide from the surface to the depths of the beginning of the Earth's crust and starting from the depth of the beginning of the Earth's lower mantle to its end.
4. The lack of clarity of the compounds actually present in the Earth's layers, due to the lack of agreement between these values between all the parameters, except for confirming the presence of iron oxide starting from a depth of 1571 km to the last depth.
5. The increase in the accuracy of the iron ratio in the studied compounds from percentage to more accurate confirms that they are mostly effective. And it's only in some very few domains, except for the density that this precision is effective on all domains.
6. Our inability to determine parameter values at the two depths, because the data from the study are decreased due to the phase transitions of this oxide occurring in this region.
7. This study can prove failure, in particular Hashin & Shtrikman's relationships to identify elastic modulus, or their validity in certain ranges.
8. The same steps can be used to study many other minerals.

REFERENCE

- Baddari, K. (1994). *Eléments de sismologie*. OPU Alger 1994, 466 P.
- Benatallah N et.al, A Computational Study to Determine and Compare the Structural and Elastic Properties of MgO, CaO and the Earth Material at PREM Pressures up to the Outer Core's Limits of the Earth, *Tobacco Regulatory Science (TRS)* (2023): 712-746.
- Bolt B and B K. *An introduction to the theory of seismology*. Cambridge University Press, Cambridge U.K., 499 pp. 1985.
- Bullen, K. E., & Bolt, B. A. (1985). *An introduction to the theory of seismology*. Cambridge university press.
- Dziewonski, A. M., & Anderson, D. L. (1981). Preliminary reference Earth model. *Physics of the earth and planetary interiors*, 25(4), 297-356.
- Jackson, I. (Ed.). (2000). *The Earth's mantle: composition, structure, and evolution*. Cambridge University Press.
- Karki BB, Stixrude L, Wentzcovitch RM. High-pressure elastic properties of major materials of Earth's mantle from first principles. *Reviews of Geophysics*. 2001;39:507-34.
- Kennett, B. L. N. (2006). On seismological reference models and the perceived nature of heterogeneity. *Physics of the Earth and Planetary Interiors*, 159(3-4), 129-139.
- Kumar, M. (2002). Application of high pressure–high temperature equation of state for elastic properties of solids. *Physica B: Condensed Matter*, 311(3-4), 340-347.
- Marx, D., & Hutter, J. (2000). Ab initio molecular dynamics: Theory and implementation. *Modern methods and algorithms of quantum chemistry*, 1(301-449), 141.
- Mattern E.. *Composition et température dans le manteau profond: interprétations minéralogiques des observations sismologiques*: Ecole Normale Supérieure de Lyon; 2005.
- Murakami M, Hirose K, Ono S, Tsuchiya T, Isshiki M, Watanuki T. High pressure and high temperature phase transitions of FeO. *Physics of the earth and planetary interiors*. 2004;146:273-82.
- Louail, L., Krachni, O., Bouguerra, A., & Sahraoui, F. A. (2006). Effect of pressure on structural and elastic properties of alkaline-earth oxide CaO. *Materials Letters*, 60(25-26), 3153-3155.
- P. Hohenberg, W. Kohn, *Phys. Rev. B* 136 (1964) 864.

- Perdew, J. P., Burke, K., & Ernzerhof, M. (1996). Generalized gradient approximation made simple. *Physical review letters*, 77(18), 3865.
- Perdew JP, Chevary JA, Vosko SH, et al. Atoms, molecules, solids, and surfaces: applications of the generalized gradient approximation for exchange and correlation. *Phys Rev B*. 1992;46:6671.
- Perdew, J. P., Ruzsinszky, A., Csonka, G. I., Vydrov, O. A., Scuseria, G. E., Constantin, L. A., ... & Burke, K. (2008). Restoring the density-gradient expansion for exchange in solids and surfaces. *Physical review letters*, 100(13), 136406.
- Perdew, J. P., & Zunger, A. (1981). Self-interaction correction to density-functional approximations for many-electron systems. *Physical Review B*, 23(10), 5048.
- Poirier, J. P. (2000). *Introduction to the Physics of the Earth's Interior*. Cambridge University Press.
- Radovic M, Lara-Curzio E, Riester L. Comparison of different experimental techniques for determination of elastic properties of solids. *Materials Science and Engineering: A*. 2004;368:56-70.
- Segall M, Lindan P, Probert M, Pickard C, Hasnip P, Clark S, Payne M. Materials Studio CASTEP Version 2.2 (2002);(b) M. Segall, P Linda, M Probert, C Pickard, P Hasnip, S Clark, M Payne, *J Phys: Condens Matter*. 2002;14:2717-44.
- Shearer, P. M. (2009). *Introduction to Seismology*, Cambridge University Press.
- Sobolev SV, Babeyko AY. Modeling of mineralogical composition, density and elastic wave velocities in anhydrous magmatic rocks. *Surveys in geophysics*. 1994;15:515-44.
- Stein, C. A. (1991). *The solid earth: an introduction to global geophysics*.
- Tlili S, Louail L, Bouguera A, Haddadi K, Medkour Y. Contribution to the study of structural and elastic properties of wüstite under pressure up to 140 GPa by pseudopotential calculations. *Phase Transitions*. 2017;90:1229-40.
- Volgyesi, L., & Moser, M. (1982). The inner structure of the Earth. *Periodica Polytechnica Chemical Engineering*, 26(3).
- Werner, W. (1984). Polynomial interpolation: Lagrange versus newton. *Mathematics of computation*, 43(167), 205-217.